A novel phenolic formulation for treating hepatic and peripheral insulin resistance by regulating GLUT4-mediated glucose uptake

Bean bu Kang [a, b], Been huang Chiang [a, *]

[a] Institute of Food Science and Technology, National Taiwan University, Taipei, Taiwan
[b] Research Institute of Liquor and Biotechnology, Taiwan Liquor Corporation, Taipei, Taiwan

ARTICLE INFO

ABSTRACT

Chronic insulin resistance suppresses muscle and liver response to insulin, which is partially due to impaired vesicle trafficking. We report here that a formula consisting of resveratrol, ferulic acid and epigallocatechin-3-O-gallate is more effective in ameliorating muscle and hepatic insulin resistance than the anti-diabetic drugs, metformin and AICAR. The formula enhanced glucose transporter-4 (GLUT4) translocation to the plasma membrane in the insulin-resistant muscle cells by regulating both insulin-independent (calcium and AMPK) and insulin-dependent (PI3K) signaling molecules. Particularly, it regulated the subcellular location of GLUT4 through endosomes to increase glucose uptake under insulin-resistant condition. Meanwhile, this phytochemicals combination increased glycogen synthesis and decreased glucose production in the insulin-resistant liver cells. On the other hand, this formula also showed anti-diabetic potential by the reduction of lipid content in the myotubes, hepatocytes, and adipocytes. This study demonstrated that the three phenolic compounds in the formula could work in distinct mechanisms and enhance both insulin-dependent and independent vesicles trafficking and glucose transport mechanisms to improve carbohydrate and lipid metabolism.

© 2021 Center for Food and Biomolecules, National Taiwan University. Production and hosting by Elsevier Taiwan LLC. This is an open access article under the CC BY-NC-ND license (http://creativecommons.org/licenses/by-nc-nd/4.0/).

1. Introduction

Chronic hyperglycemia resulting from insulin resistance has been an important health issue worldwide. Insulin resistance associated with type 2 diabetes mellitus (T2DM) is mostly seen in peripheral organs, including skeletal muscle, liver, and adipose tissue.[1] Glucose uptake and glycogen synthesis in skeletal muscle are particularly important, which is responsible for more than 70 % of total body glucose disposal.[2] The liver maintains blood glucose levels by balancing glucose uptake and storage via glycogenesis and glucose production via gluconeogenesis.[3] Lipogenesis and lipolysis in adipocytes control energy balance and glucose homeostasis.[4] All three organs are of particular relevance due to their crucial roles in glucose metabolism and the development of T2DM. This fact would have a considerable clinical significance because it can be seen as a whole management system to reduce the severity of hyperglycemia and lipid dysregulation through increasing glucose use, suppressing glucose production, or elevating energy expenditure.

Elevated free fatty acid (FFA) level is a clinically relevant cause of insulin resistance and T2DM.[5] Acute elevations of plasma FFA levels, for instance by saturated and monounsaturated fatty acids intake, are the main causative factor of metabolic syndrome.[6] The fatty acid intermediates are associated with the progression of insulin resistance in insulin-sensitive tissues, targeting and hampering specific actors of the insulin signaling pathway.[7] Insulin resistance may also be related to the increased intramyocellular

neutral lipid accumulation and incomplete fatty acid oxidation.[8] A commonly pharmacological agent for the treatment of insulin resistance is 1,1-dimethylbiguanide hydrochloride (metformin), an orally administered drug that exhibits potent insulin-sensitizing properties and decreases blood sugar in individuals with T2DM. Metformin enhances glucose uptake by a mechanism largely independent of 5′-adenosine monophosphate-activated protein kinase (AMPK).[9] It has been proposed that metformin attenuates FFA-induced insulin resistance by augmenting the insulin signaling pathway and AMPK pathway.[7] Other than lowering blood glucose level, metformin was also found to be able to reduce the adipose tissue weight by downregulating adipogenesis.[10] Another potential drug for treating diabetes is 5-aminoimidazole-4-carboxamide ribonucleotide (AICAR). It is an AMPK activator but not allowed to be used due to the potential performance-enhancing effect.

Phytochemical-based anti-diabetic diets and nutraceutical formulation have been a modern management of insulin resistance and related conditions.[11–15] Some phytochemicals, e.g. flavonoid, phenolic acid, and stilbene, are able to regulate glucose uptake in muscle, hepatic and adipose cells through the insulin-independent pathway.[15–17] Ferulic acid (FER), the single phenol compound can simultaneously decrease blood glucose in C57BL/KsJ-db/db mice and high-fat diet-induced type 2 diabetic rats,[18,19] indicating that phenolic acids increases glucose transporter-4 (GLUT4) translocation-mediated glucose uptake and glycogen synthesis together with reducing glucose production and fat deposition via phosphoinositide 3-kinase (PI3K)/AKT pathway in peripheral tissues.[20] Resveratrol (RSV), the double phenol compound was found to activate cAMP-AMPK signaling pathway and promote glucose utilization as well as lower lipid accumulation, has been proposed as a possible caloric restriction mimetic based on its ability to combat high fat-induced insulin resistance.[21–23] Epigallocatechin-3-*O*-gallate (EGCG), the complex phenolic compound popularly found in tea, increases lipid oxidation and glucose uptake by activating AMPK, while improving blood glucose homeostasis and inhibiting lipogenesis in insulin-resistant diabetic animal models.[15,21,24,25]

Although evidences showed that different phenolic compounds act through distinct mechanisms to ameliorate insulin resistance, the specific underlying complementary and synergistic properties of these phytochemicals that may contribute to the improvement of insulin resistance have not yet been identified. This study proposed that the combination of one, two and complex six-carbon ring structures will act synergistically to enhance glucose disposal and reduce lipid accumulation, thereby causing an overall improvement of systemic insulin resistance. To prove this hypothesis, vesicle trafficking, glucose transporter translocation, glucose uptake, glycogen synthesis, glucose production, and lipid accumulation in FFA-induced peripheral insulin resistance were analyzed. Once this hypothesis is proved, the potential of the phytochemical combination for enhancing the glucose transporter-containing vesicle trafficking via insulin-independent pathway could be fully understood, which in turn could control disease conditions related to insulin resistance, such as T2DM, obesity, and hepatic steatosis.

2. Materials and methods

2.1. Materials

Rat myoblast-like cells (L6 cell line) originally isolated from primary cultures of rat thigh were purchased from Japan Health Sciences Foundation, Health Science Research Resources Bank (Osaka, Japan). Human hepatocellular liver carcinoma (HepG2 cell line) and mouse preadipocyte (3T3-L1 cell line) were obtained from the Bioresources Collection and Research Center of Food Industry Research and Development Institute (Hsinchu, Taiwan). Mouse

monoclonal antibody against GLUT4 (clone 1F8) was purchased from R&D Systems (Minneapolis, MN, USA). Rabbit polyclonal anti-phospho-AKT antibody (Thr305/308/309) was purchased from Bioss (Beijing, China). Mouse monoclonal anti-phospho-Acetyl CoA Carboxylase (Ser79) and anti-β-actin (A2228) were purchased from Sigma Aldrich (St. Louis MO, USA). All other chemicals, including FER (PubChem CID: 445858), RSV (PubChem CID: 445154), EGCG (PubChem CID: 65064), metformin (PubChem CID: 14219), AICAR (PubChem CID: 266934), DMSO (dimethyl sulfoxide) (PubChem CID: 679), palmitate (PubChem CID: 16218516), oleic acid (PubChem CID: 445639), 2-deoxyglucose (2DG) (PubChem CID: 439268), indinavir (IDV) (PubChem CID: 5484730), BAPTA-AM (PubChem CID: 2293), Compound C (PubChem CID: 11524144), LY294002 (PubChem CID: 3973), cytochalasin B (CB) (PubChem CID: 6916220), were purchased from Sigma-Aldrich (St. Louis, MO, USA) unless otherwise specified; all buffers and aqueous solutions were prepared using sterile deionized water. FER, RSV and EGCG were dissolved in DMSO.

2.2. Muscle tissue collection and incubation

Male C57BL/6 mice (NAR Labs, Taiwan) weighing 19–24 g were maintained on a 12 h light-dark cycle in a temperature-controlled environment (25 °C) and allowed free access to standard rodent chow diet (Laboratory Rodent Diet 5001, LabDiet, St. Louis, MO) and fasted overnight prior to the experiment, but allowed free access to water. The Ethics Committee on Animal Research in National Taiwan University approved. The mice were humanely killed by CO_2 asphyxiation.

The forelimb epitrochlearis and hindlimb soleus muscles were carefully removed and rapidly rinsed in phosphate-buffered saline (PBS) for *in vitro* incubation immediately after sacrifice as previous described.[26] The muscles were longitudinally split into strips of similar size for each muscle and incubated with shaking at 37 °C in pre-gased (95 % O_2, 5 % CO_2) Krebs-Henseleit buffer (KHB) containing 0.1 % bovine serum albumin (BSA). The incubated muscles were transferred to fresh KHB and incubated with either insulin (100 nM) or various test compounds as described in the figure's legends.

2.3. Cell culture and treatment

L6 rat skeletal muscle cells were maintained as described previously.[27] For differentiation into myotubes, L6 myoblasts were seeded in multiwell plates at the density of 6×10^4 cells/cm^2 in Dulbecco's modified Eagle's medium (DMEM) supplemented with 10 % fetal bovine serum (FBS) at 37 °C in a humidified atmosphere of 5 % CO_2. After 2 days, the medium was replaced with α-minimal essential medium (α-MEM) supplemented with 2 % FBS. At 5 days of differentiation, myotubes were treated with medium containing 0.75 mM palmitate, 1 % BSA, and 2 % FBS for 16 h followed by 18-h period in serum-free medium. The cells were then used for different assays as detailed below.

Cells from a human, well differentiated hepatocellular liver carcinoma cell line, HepG2, were cultured as previously described.[28] For the experiments, HepG2 cells were seeded at 3×10^4 cells/well in 96-well plate and incubated with 10 % FBS/DMEM. When cells reached about 80 % confluence, cultured cells were treated with FFA, including 0.75 mM palmitate (saturated) or 1 mM oleate (one double bond), in media containing 1 % BSA for 24 h. Subsequently, the experiments were performed as indicated in the figure's legend.

Murine 3T3-L1 preadipocytes were subcultured in six-well plates at a density of 5×10^3 cells/well in DMEM supplemented with 10 % FBS. Differentiation was induced after reaching

confluence. To differentiate the cells to adipocytes, the method described by Fazakerley et al. was used.[29] During differentiation, the cells were treated with phytochemicals every 3 d at the concentrations indicated in figure. Control cells were incubated in medium containing the same amount of DMSO, as 0.1 %.

2.4. Endosome ablation using HRP-conjugated transferrin

Transferrin conjugated to horseradish peroxidase (Tf-HRP) was used as previously described with some modifications.[30] Palmitate-treated L6 myotubes were washed twice with Krebs–Ringer phosphate-HEPES buffer (KRH; 50 mM HEPES, pH 7.4, 137 mM NaCl, 4.8 mM KCl, 1.85 mM $CaCl_2$, 1.3 mM $MgSO_4$) containing 0.1 % BSA for 1 h at 37 °C under 5 % CO_2 in the presence of 20 μg/mL Tf-HRP which was prepared by the carbodiimide method and purified as described.[31] Cells were washed with ice-cold isotonic citrate buffer (150 mM NaCl, 20 mM sodium citrate, pH 5.0) to remove excess ligand and reequilibrated with ice-cold PBS (pH 7.4) for 15 min on ice. Endosome ablation by diaminobenzidine (DAB) polymerization was done by incubating cells in 100 μg/mL DAB plus 0.02 % H_2O_2 diluted in 0.1 % (w/v) BSA/KRH buffer for 60 min at 4 °C in the dark. The reaction mixture was quenched by exposure to KRH buffer containing 5 mg/mL BSA. Cells were washed twice and immediately used for experiments.

2.5. Measurement of glucose uptake

Indicated cells were washed and exposed to 0.1 % (w/v) BSA buffer in the absence or presence of the various inhibitors followed by a 15-min incubation in fresh 0.1 % (w/v) BSA buffer containing test compound or vehicle at 37 °C. After this, they were incubated for 20 min at 37 °C in 0.1 % (w/v) BSA buffer containing 2DG and continuous gas phase of 95 % O_2, 5 % CO_2. The cells were subsequently washed with ice-cold PBS 5 times and lysed in 0.1 N NaOH. Glucose uptake activity was analyzed by the accumulation of intracellular 2DG6P as described previously.[32]

2.6. Subcellular fractionation, gel electrophoresis, and immunoblotting

GLUT4 translocation assay was conducted as described previously with some modifications.[33] The cells were washed with KRH buffer, then homogenized with lysing buffer (50 mM Tris, pH 8.0, 0.1 % v/v Nonidet P-40, 0.5 mM dithiothreitol) containing Complete protease inhibitor mixture (Roche) by passing through 27-gauge needles prior to centrifugation. The precipitate obtained after centrifugation was suspended again in lysing buffer and homogenized again. After centrifugation, the pellet was washed with Nonidet P-40-free lysing buffer and spun. The as-obtained precipitate was resuspended with lysing buffer for 1 h. This suspension was centrifuged and the supernatant was used as the plasma membrane (PM) fraction. The mixed supernatant from the first and second centrifugation was centrifuged and the supernatant was used as the post-PM fraction. 10 μg of protein were then separated by sodium dodecyl sulfate polyacrylamide gel electrophoresis (SDS-PAGE) and electrotransferred to polyvinylidene difluoride (PVDF) membranes as described.[29] The blocked filters were incubated with mouse monoclonal or rabbit polyclonal antibodies, washed extensively, and the immunoreactive band was visualized with HRP-conjugated goat anti-mouse or anti-rabbit IgG for polyclonal antibodies, by means of an enhanced chemiluminescence (ECL) detection technique.

2.7. Measurement of glucose output

Cellular glucose production in HepG2 was used to evaluate gluconeogenesis as previously published with some modifications.[34] The cells were incubated at 37 °C in glucose production buffer of glucose-free Dulbecco's modified essential medium (pH 7.4) without phenol red supplemented with 10 mM sodium lactate, 1 mM sodium pyruvate, 100 nM dexamethasone, 100 μM dibutyryl cAMP (Bt2-cAMP), 2 mM L-glutamine, 44 mM sodium bicarbonate and 15 mM HEPES. After 3 h of incubation, the medium was collected and glucose concentration was determined.

2.8. Analysis of glycogen contents

Hepatic glycogen was hydrolyzed to glucose with an amylo-glucosidase.[35] The cells were incubated with 5 mM glucose for 3 h at 37 °C, homogenized in 0.6 N $HClO_4$. Immediately thereafter the homogenate was neutralized with 1 M $KHCO_3$, glycogen was degraded with 10 mg/mL amyloglucosidase in 0.2 M acetate buffer (pH 4.8) for 2 h at 40 °C, and chilled 2 N $HClO_4$ was added to stop the reaction. After centrifugation at 14,000 g at 4 °C for 10 min, the supernatant was collected for determination of glucose concentration.

2.9. Determination of cellular lipid accumulation

After the indicated incubations, cells were fixed in 10 % formalin in PBS for 60 min and excess of formaldehyde was removed by three rinses in distilled water for 30 s. As described previously,[36] cells were stained with 0.2 % freshly filtered Oil Red O (ORO) working solution per well at room temperature for 40 min. Subsequently, cells were then washed with deionized water per well three times and then washed with 60 % isopropanol to remove unbound dye. After the cells were dried, the stained lipid droplets were extracted using isopropanol for 30 min at room temperature. Finally, the absorbance was measured at 405 nm with a microplate reader (Thermo Fisher Scientific, Finland) and blanked to cell-free well. Stained lipid droplets were observed for histological study using an inverted phase contrast microscope (Olympus CKX41) and photo-micrographed with the help of digital camera (Bestscope BHC2–1080P).

2.10. Statistical analysis

Data are given as mean ± standard deviation (SD) of the indicated number of measurements. The significant results of analysis of variance (ANOVA) were analyzed using Tukey's *post hoc* honest significant difference (HSD) test. Treatment effects were evaluated using a two-tailed Student's *t*-test. A probability value of $p < 0.05$ was considered statistically significant. For each figure, the statistical significance was specified in the legend.

3. Results and discussion

3.1. The combination of selected phytochemicals elicits glucose uptake in normal muscle cells

It has been reported that skeletal muscle has important roles in maintaining glucose homeostasis, and insulin resistance involves defective glucose transport in skeletal muscle.[37] The first stage of this research was designed to use primary skeletal muscle cells as a cell culture model. The non-immortalized cells allowed us to increase the relevance of our results to actual muscle. Insulin resistance occurs more seriously in fast-twitch myofibers which have lower oxidative capacity,[37] but the slow-twitch myofibers have also

been demonstrated to become insulin resistant for glucose uptake.[26] Since both soleus (slow-twitch) and epitrochlearis (fast-twitch) were found to be able to increase glucose transport in response to various phenolic compounds,[38,39] we first evaluated the effect of phenolic combination on the glucose uptake by these two normal muscle cells. As shown in Fig. 1, the phenolic combination induced significant increases in glucose uptake in both of these primary muscle fibers. However, there was no significant difference in glucose uptake by these two muscles regardless of their different twitching ability. Besides, no significant differences were observed among the phenolic combination, insulin, and the anti-diabetic drugs, metformin and AICAR, indicating that in normal muscle cells, the phenolic combination had the same eliciting effect on glucose uptake as insulin and anti-diabetic drugs.

Metformin enhances glucose uptake in skeletal muscle cells by a mechanism largely independent of AMPK, it acts via non-AMPK pathways.[9] The AICAR, on the other hand, is an AMPK activator.[40] The hexose transport in the isolated muscle reflects the muscle' intrinsic carbohydrate metabolism as well as the prior *in vivo* condition. The similar glucose uptake ability of these two different muscles in responding to the anti-diabetic drugs and phenolic combination suggested that their glucose-uptake promoting activity are the same in different fiber-type muscles. In addition, these results also suggested that the phenolic combination has similar function as the anti-diabetic drugs, regardless of their different mode of action in muscle.

3.2. Phenolic combination increases GLUT4 translocation in insulin-resistant muscle cells

Delivery of GLUT4 to the PM in response to insulin increases glucose uptake.[41] We compared the glucose-uptake stimulating ability of our phenolic combination with insulin and anti-diabetic drugs upon the palmitate-induced insulin-resistant muscle cells, and the results is shown in Fig. 2. The phenolic combination exhibited a superior ability of enhancing glucose uptake, it is not only better than insulin but also more effective than the anti-

diabetic drugs, including metformin and AICAR. Furthermore, we investigated the role of GLUT4 in this glucose-uptake stimulating study using IDV. IDV, a protease inhibitor, selectively blocks glucose uptake by inhibiting GLUT4 in L6 muscle cells.[42] We found that the positive effect of phenolic combination on glucose uptake was blocked in the IDV-pretreated cells, and the difference among phenolic combination, insulin, and anti-diabetic drugs disappeared (Fig. 2). These results suggested that the phenolic combination and anti-diabetic drugs stimulated glucose uptake in the insulin-resistant muscle cells in a similar way, and the mechanism involves GLUT4.

The increase in skeletal muscle glucose uptake is mediated by the translocation of GLUT4 to the PM, which is known to play an important role in the maintenance of body glucose homeostasis.[1] L6 muscle cells express GLUT4 specifically. Therefore, we further examined the distribution of GLUT4 protein in different cellular fractions prepared from lysates of palmitate-treated myotubes. As shown in Fig. 3, GLUT4 was translocated to the PM upon insulin stimulation, confirming the results from earlier studies.[1] In fact, the insulin, phenolic combination and the anti-diabetic drugs metformin all increased the presence of GLUT4 protein in the PM. It is worthy of noting that the increase in GLUT4 protein and Ser 79 phosphorylation of acetyl-CoA carboxylase (ACC), downstream targets of AMPK, in response to the phenolic combination appeared to be greater than the anti-diabetic drugs, metformin and AICAR. The protein level of phosphorylated AKT, the protein activated by PI3K, was also upregulated by the phytochemical combination in our insulin-resistant model. Since the AKT signaling was impaired under insulin-resistant condition, the immunoblotting showed that the phytochemical combination could only weakly upregulate this protein.

3.3. Phenolic combination stimulates glucose uptake through PI3K and AMPK pathways in insulin-resistant muscle cells

In order to better understand the mechanism through which the EGCG and/or resveratrol and/or ferulic acid act on glucose
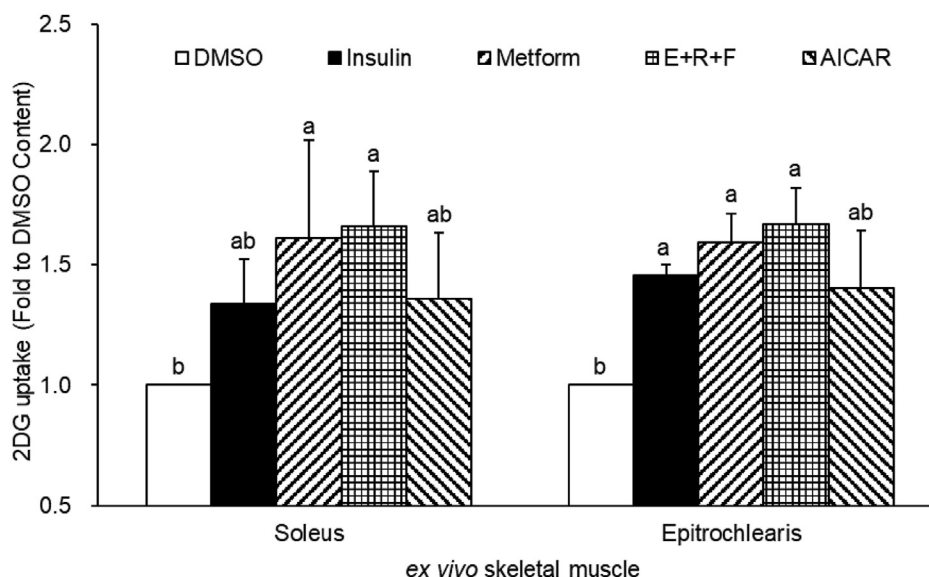

Fig. 1. Comparison of the glucose-uptake-stimulating efficacy of phenolic combination and anti-diabetic drugs in soleus and epitrochlearis muscle. Muscle were initially incubated at 35 °C for 60 min in KRH buffer before being treated with DMSO (0.1 %, control), insulin (100 nM) or AICAR (2 mM) or metformin (1 mM) or combination of FER (25 μM) and RSV (10 μM) and EGCG (5 μM) for 15 min. Glucose uptake activity was then assessed by measuring the intracellular accumulation of 2DG at 35 °C for 20 min 2DG uptake was determined as described previously. Relative activity was calculated as the ratio of 2DG uptake in test compounds-treated L6 myotubes to that in DMSO-treated cells. Values are means ± SD for 5 muscles per group. Statistical analysis was performed using two-tailed unpaired Student's *t*-tests (*$p < 0.05$) compared with insulin-treated cells.
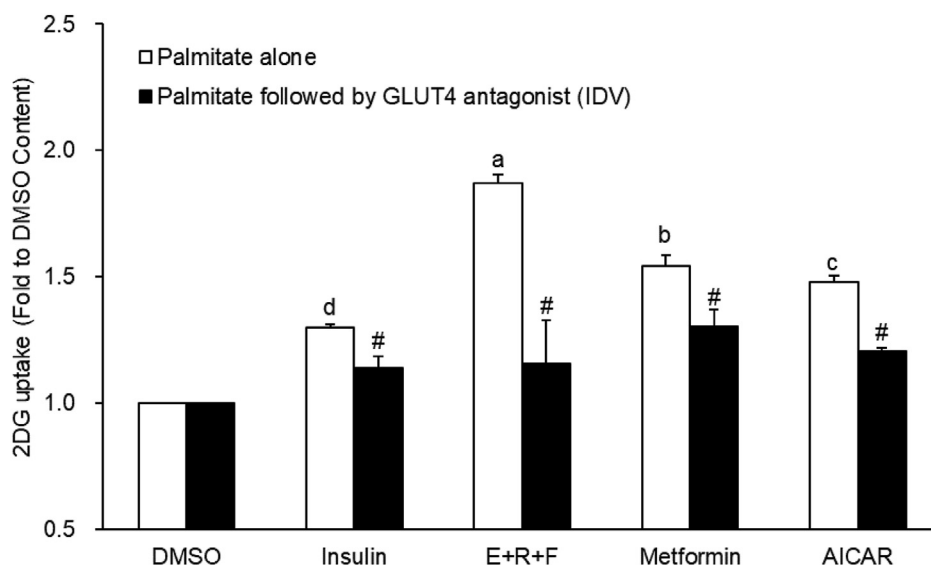
Fig. 2. Effect of phenolic combination and anti-diabetic drugs on IDV-pretreated insulin-resistant L6 myotubes. Palmitate-treated L6 myotubes were stimulated for 5 min without or with 100 µM IDV, then incubated with DMSO (0.1 %), phenolic combination (5 µM EGEG + 10 µM RSV + 25 µM FER), metformin (1 mM) or AICAR (2 mM) for 15 min. Data present the 2DG uptake influenced by palmitate pretreatment only (white bars) and palmitate along with IDV treatment (closed bars). Results are the means +SD of five independent experiments. Different superscript letters indicate significant differences at $p < 0.05$. The GLUT4 dependent effect above basal was calculated for each stimulator. $^{\#}p < 0.05$ compared with GLUT4 effect in cells not treated with IDV.
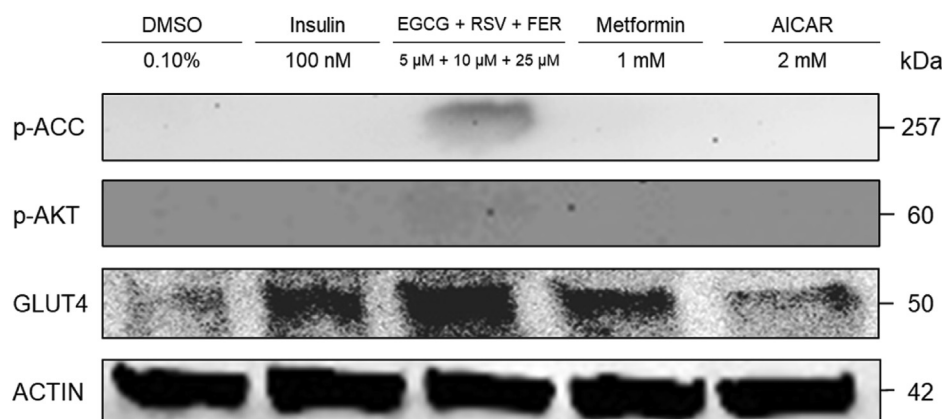

Fig. 3. Effect of phenolic combination and anti-diabetic drugs on the translocation of GLUT4 to plasma membrane and the related intracellular signaling molecules including phosphorylated AKT (*p*-AKT) and ACC (*p*-ACC) in insulin-resistant L6 myotubes. Palmitate-treated myotubes were incubated with DMSO (0.1 %), phenolic combination (5 µM EGEG + 10 µM RSV + 25 µM FER), metformin (1 mM) or AICAR (2 mM) for 15 min. The cell lysates were used for preparation of a plasma membrane fraction as described under "Methods". Protein (50 µg) was resolved by SDS-PAGE and Western blotted for the proteins shown. Detection was by enhanced chemiluminescence, and a representative blot is depicted. Anti-β-actin was used as protein loading control of whole homogenate.

metabolism, we further explored their vesicle trafficking and signaling cascades in palmitate-treated skeletal muscle cells. As shown in Fig. 4, all of these phytochemicals can stimulate glucose uptake in palmitate-treated myotubes, however, the positive effects of them were blocked by BAPTA-AM (an intracellular calcium chelator) or Compound C (an AMPK inhibitor). Interestingly, ablation of recycling endosome significantly decreased the glucose uptake elicited by the phenolic combination. This raised the question whether blocking the non-endosomal GSVs trafficking using PI3K inhibitor LY294002 would also decrease glucose uptake of the phenolic combination treated insulin-resistant muscle cells. The results showed that LY294002 indeed inhibited the phenolic combination stimulation effect on insulin-resistant muscle cells (Fig. 4). Thus, the phenolic combination boosted both endosome and GSVs trafficking under an insulin-resistant state. The insulin-independent therapeutic effect appeared to make a relatively large contribution toward the overall increase in glucose uptake elicited by the phenolic compounds. The phenolic combination appeared to be able to stimulate glucose uptake in insulin-resistant muscle cells via differential targeting of different subcellular pools of mediators. And this gives new insight into the links between signaling, vesicle trafficking and insulin resistance.

Insulin stimulated glucose uptake is most pronounced in muscle cells. The insulin/PI3K/AKT signaling cascade is most likely active and probably not the only active signaling pathway governing the trafficking of GLUT-positive vesicles to the PM and glucose uptake.[43,44] Intracellular calcium and AMPK also acts on the vesicle trafficking pathway,[45] that transports GLUT4 from the GSVs or endosome to the PM.[46] The rat skeletal muscle cell line L6 is considered a good *in vitro* model because the results are representative of glucose flux regulation *in vivo*.[47] By using chemical ablation to block the TfR-positive glucose transporter containing
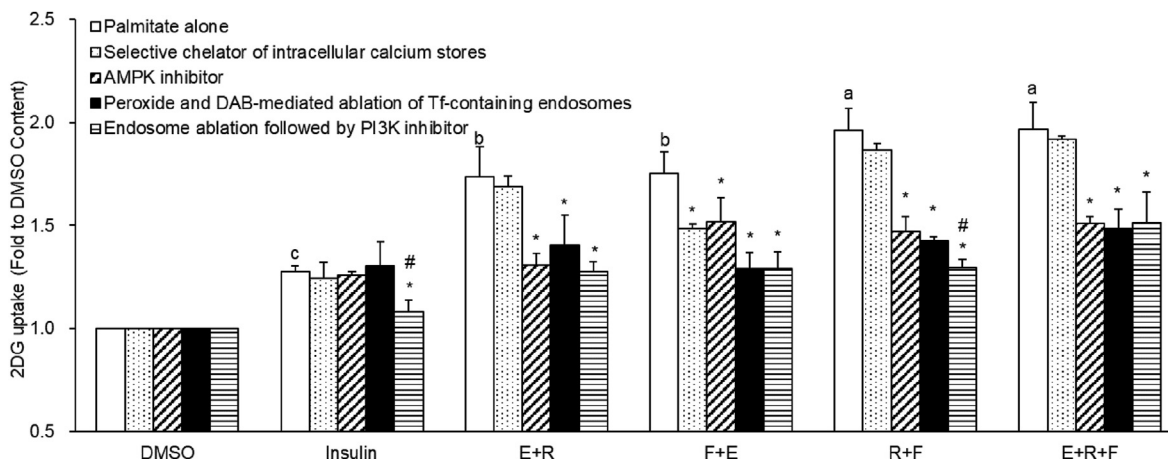
Fig. 4. Effects of endosome ablation and inhibitors on phenolic combination-stimulated glucose uptake. Differentiated L6 cells in 96-well plate were cultured in the presence of 0.75 mM palmitate for 14 h, and then kept in serum-starved medium without palmitate for a further 18 h. These myotubes were incubated with 50 μM BAPTA-AM or 20 μM Compound C for 30 min. Some cells were also incubated with 20 μg/mL Tf-HRP for 60 min and DAB cytochemistry reaction was then performed in presence of hydrogen peroxide. After ablation, cells were washed once in ice-cold PBS containing 5 mg/mL BSA, and then incubated with 25 μM LY294002 for 5 min. They were then treated with DMSO (0.1 %, control), EGCG (25 μM) and/or resveratrol (10 μM) and/or ferulic acid (25 μM) for another 15 min, and finally incubated in 2DG-containing buffer for a further 20 min. The uptake of 2DG was determined using an enzymatic, fluorescent method. Relative activity was calculated as the ratio of 2DG uptake in phytochemicals-treated L6 myotubes to that in DMSO-treated cells. Data are shown as the mean +SD form five independent experiments. Means in each column not sharing a common superscript letter are significantly different ($p < 0.05$). Statistical analysis was performed using two-tailed unpaired Student's t-tests (*$p < 0.05$) compared with endosome-unablated cells; (#$p < 0.05$) compared with inhibitor-untreated cells. E, EGCG; R, Resveratrol; F, Ferulic acid; 2DG, 2-deoxyglucose.

vesicles,[48,49] we demonstrated that the phenolic combination with EGCG, RSV and FER can improve glucose uptake in insulin-resistant skeletal muscle (Fig. 4), and the beneficial effect of phenolic combination on insulin resistance may be mediated through the insulin-independent mechanisms such as regulating the calcium pool, stimulating AMPK, and improving endosome trafficking in muscle. Therefore, it could be suggested that the chemical structure of the polyphenols may play an important role in the modulation of cell signaling and vesicle trafficking. The AMPK pathway is targeted in RSV and EGCG action. The galloyl moieties of EGCG (epi-gallocatechin-3-gallate) could contribute to the stimulation of endosomal AMPK. The structure of resveratrol (3,5,4′-trihydroxy-trans-stilbene) contains a central carbon-carbon double bond. This double bond may be related to its manipulation of GSVs. Ferulic acid (3-methoxy-4-hydroxycinnamic acid) targeting the PI3K pathway in muscle cells might be due to its guaiacyl moiety (vicinal OH and OCH$_3$ group). This study also demonstrated the independent roles of FER, RSV and EGCG in regulating glucose utilization in muscle cells, with favoring insulin-independent signaling and vesicle trafficking in L6 muscle cells (Fig. 4). We suggest that these phenolic compounds can synergistically enhance glucose transport due to the complementary of the endosome and GSVs trafficking in PI3K and AMPK signaling pathways.

3.4. Phenolic combination promotes glucose metabolism more effectively than the anti-diabetic drugs in hepatocytes

In dietary polyphenols-treated cafeteria diet-induced rat model of metabolic syndrome, non-alcoholic fatty liver disease progression was strongly retarded.[50] To extend the observations from myotubes to hepatic insulin resistance, the human hepatocyte cell line HepG2 were treated with the same concentrations of palmitate and assessed their glucose uptake activity. Fig. 5A shows that glucose uptake was elevated in response to phenolic combination, metformin, and AICAR. The phenolic combination appeared to be a more potent stimulator than the anti-diabetic drugs ($p < 0.05$). However, the glucose-uptake stimulation by either phenolic

combination or anti-diabetic drugs were suppressed in the GLUT-blocked cells.

It is known that regulation of hepatic gluconeogenesis is another regulatory role in maintaining blood glucose homeostasis.[51] Exposure of metformin and phenolic combination significantly suppressed gluconeogenesis in FFA-treated HepG2 cells, as shown in Fig. 5B. However, the decreased hepatic gluconeogenesis was completely abolished by inhibiting AMPK using Compound C, indicating that phenolic combination-stimulated glucose metabolism in liver cells has an AMPK-dependent component.

The hepatic insulin resistance in non-alcoholic fatty liver disease often leads to an increased gluconeogenesis as well as an impaired glycogen synthesis.[52] Next, we sought to determine whether the glycogen synthesis is also altered due to the treatments. We found that the levels of glycogen were obviously increased due to stimulation with phenolic combination and anti-diabetic drugs (Fig. 5C). Again, the combination of FER, EGCG and RSV caused the largest increase in glycogen accumulation in the insulin-resistant HepG2 cells.

Liver regulates blood sugar through gluconeogenesis and glycogen synthesis. Impaired hepatic insulin action leads to metabolic changes such as increased gluconeogenesis, decreased glycogen storage, and elevated fatty acid synthesis.[51] Elevated FFAs was reported to rapidly impair the ability of insulin to suppress hepatic glucose output.[53] Activation of AMPK contributed to the molecular mechanism through which the phenolic combination improved glucose uptake in muscle cells (Fig. 4) and gluconeogenesis in liver cells (Fig. 5B). AMPK has previously been shown to be a metabolic sensor that plays an important role in whole body energy balance, such as glucose uptake,[9] glucose production[54,55] and lipid metabolism.[55,56] Results of this study demonstrated that the phenolic combination regulates glucose metabolism by the reduction of hepatic gluconeogenesis and glucose uptake by muscle cells as well as by liver cells, via glycogen storage. However, the possible limitation is the expression of metabolic profiles in HepG2 cells is lower than that in human liver. Primary hepatocyte cultures from type 2 diabetic liver will be considered in our future work.
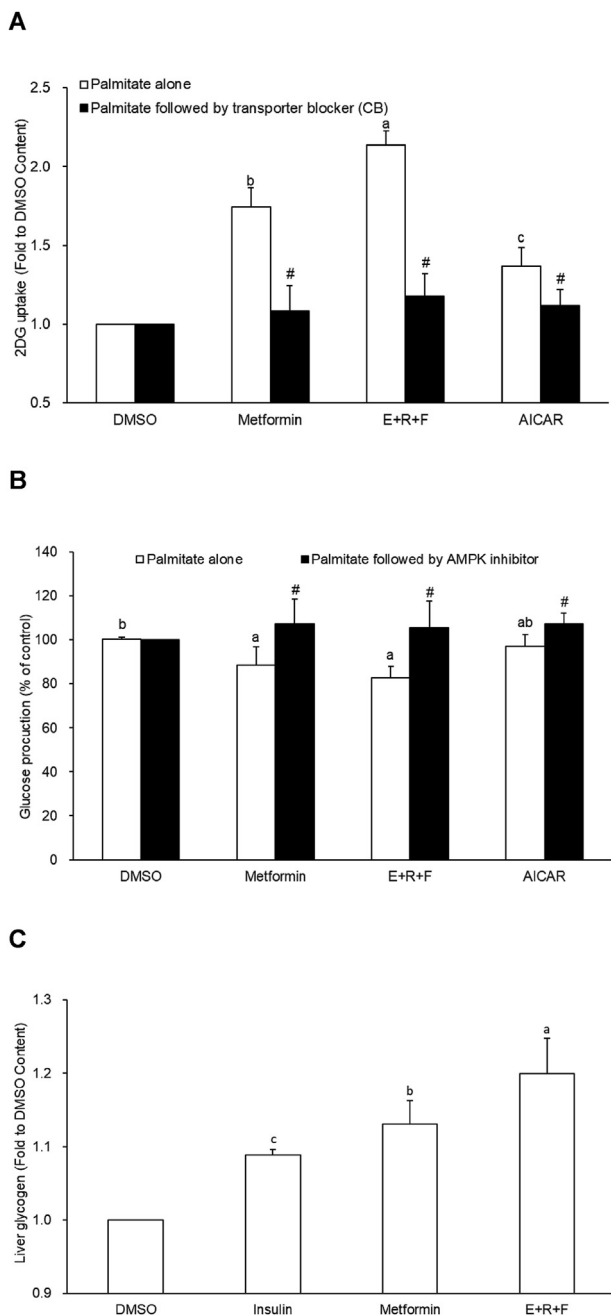
A

B

C

Fig. 5. Effect of phenolic combination and anti-diabetic drugs on glucose metabolism in insulin-resistant hepatocytes. (A) Effect on glucose uptake. Palmitate-treated HepG2 cells were incubated with DMSO, metformin, phenolic combination or AICAR prior to assaying 2DG uptake. Shown are palmitate pretreatment 2DG uptake values (white bars). Non-GLUT dependent 2DG uptake (closed bars) was measured in the presence of 10 μM cytochalasin B in the transport solution. $^{\#}p < 0.05$ compared with glucose uptake in cells in the absence of cytochalasin B. (B) Effect on glucose production. Palmitate-treated HepG2 cells were cultured in serum-free DMEM with or without 20 μM Compound C for 30 min, then in response to acute test compounds. Cells were washed twice in phosphate-buffered saline and were incubated in glucose production buffer for 3 h, after which the medium was collected for glucose measurement. Shown are palmitate pretreatment (white bars) and along with Compound C-inhibited glucose output values (closed bars). $\#p < 0.05$ compared with glucose uptake in cells in the absence of Compound C. (C) Effect on glycogen synthesis. Palmitate-treated HepG2 cells were treated with insulin, metformin or phytochemical either alone or in combination for 15 min. Cells were washed twice in phosphate-buffered saline and were subsequently incubated in serum-free DMEM for 3 h and analyzed for glycogen content. Data are shown as the mean +SD form more than five independent experiments. Statistical analysis was performed using two-tailed unpaired Student's t-tests ($^{*}p < 0.05$) compared with insulin-treated cells. Different superscript letters indicate

3.5. Phenolic combination improves lipids metabolism more effectively than the anti-diabetic drugs

Metformin and AICAR have been shown to suppress hepatic lipogenesis.[55] Plant-derived polyphenols have been proven effective in the treatment of metabolic syndromes and fatty liver.[23] In this study, we examined whether phenolic combination also leads to decreased lipid synthesis in palmitate-treated HepG2 cells. In keeping with this notion, we observed that treatment of insulin-resistant hepatocytes with either metformin or AICAR resulted in decreased lipid content (Fig. 6A). Indeed, like them, phenolic combination also prevented lipid accumulation in the insulin-resistant hepatocytes. These results suggested that the dysregulation of lipid metabolism in palmitate-treated HepG2 cells were rescued via phytochemicals-mediated glucose metabolism.

ORO and hematoxylin staining of liver sections demonstrated polyphenol-rich diets could attenuates high-carbohydrate, high-fat diet–induced liver and metabolic changes in rats.[50] Since oleate induces more cytosolic lipid droplets than palmitate,[57] we also used oleate to induce steatosis to confirm the benefit of the phenolic combination. We found that the oleate-induced steatosis in HepG2 cells was substantially inhibited by the phenolic combination, whereas AICAR was less effective (Fig. 6A). Collectively, these data suggested that the adverse events in high fat diet-induced or obesity-induced fatty liver could potentially be alleviated by the use of dietary phytochemicals.

We further investigated whether the phenolic combination can reduce fat accumulation in skeletal muscle cells. Exogenous palmitate overload leads to insulin resistance accompanied by the downregulation of several proteins associated with lipid droplet esterification, lipolysis, and oxidation.[58] Early report suggested that increases in intracellular calcium stimulates lipogenesis and inhibits lipolysis via a calcium-dependent mechanism in muscle[59] and increases mitochondrial biogenesis in L6 myotubes.[40] Effect of the phenolic combination on the intramyocellular lipid (IMCL) accumulation was evaluated in L6 myotubes after 4 h of incubation.[60] It was observed that only the phenolic combination reduced the lipid level significantly in the muscle cells (Fig. 6B). There were no significant difference in lipid accumulation in the muscle cells treated with metformin and insulin ($p > 0.05$). The lipid level in the muscle cells treated with AICAR was even significantly higher than that treated with insulin ($p < 0.05$). Thus, enhancing vesicle trafficking and the resulting improvements in glucose utilization in skeletal muscle may also improve lipid metabolism. Data from the present study demonstrated that these phenolic compounds may prevent palmitate-mediated de novo lipogenesis and insulin resistance, or increase mitochondrial biogenesis in myotubes, thereby attenuate the increase in obesity associated with T2DM.

3.6. Phenolic combination inhibits lipogenesis in 3T3-L1 adipocyte

After the study of lipid accumulation in hepatic and muscle cells, we were interested to know whether the phenolic combination will affect adipogenesis. Therefore, an in vitro study using pre-adipocytes (3T3-L1 cells) were carried out following the protocol reported by Haberland, Carrer, Mokalled, Montgomery & Olson.[61] As shown in Fig. 7A and B, treating the 3T3-L1 cells with 20 and 40 μM of phenolic combination led to significant decrease in intracellular lipid accumulation. Thus, we confirmed that phenolic combination can block adipogenesis.

Adipose tissue also develops lipogenesis leads to excessive FFA

significant differences at $p < 0.05$ using one-way ANOVA followed by the Tukey's *post hoc* comparison test.
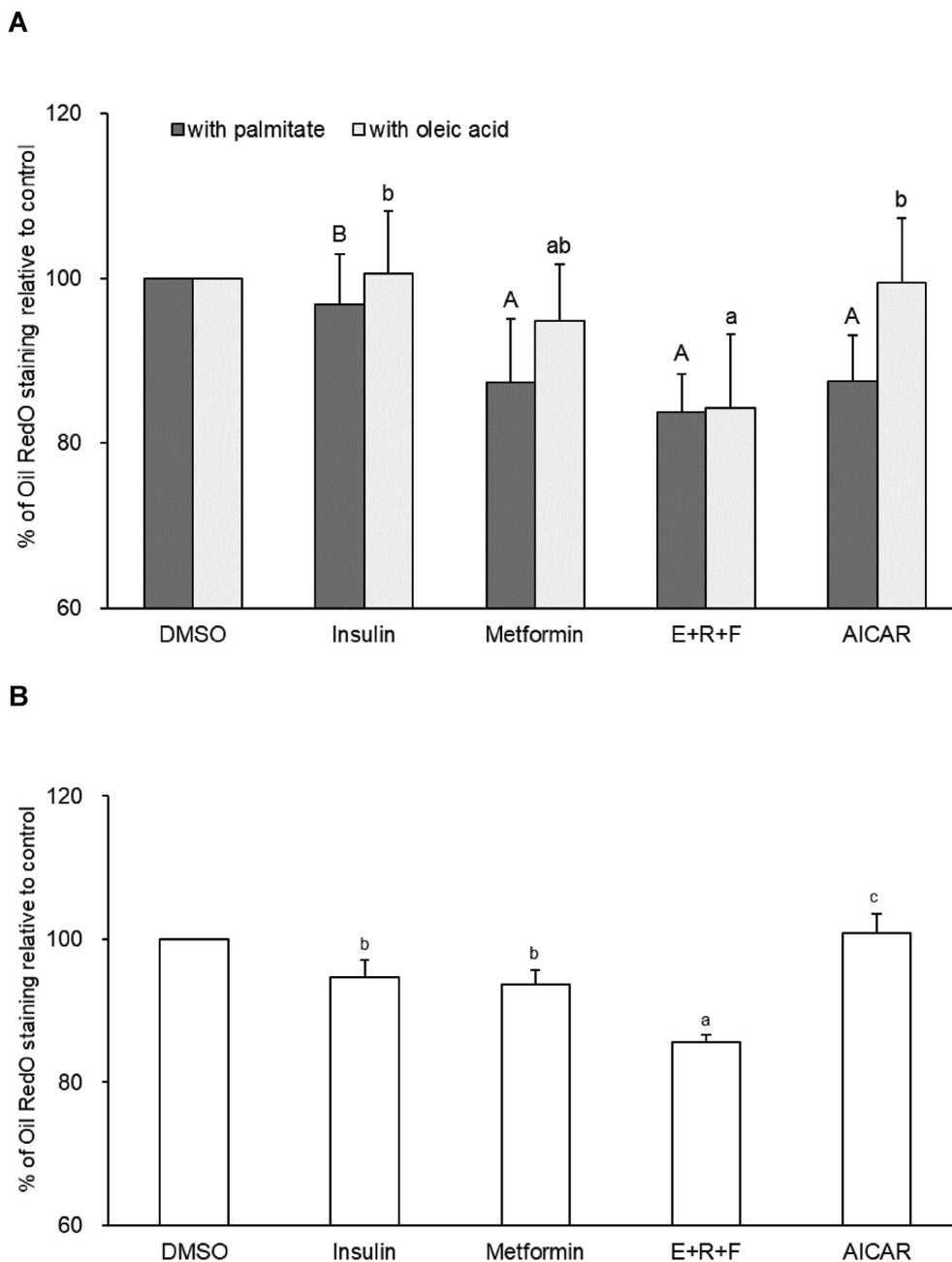
A

B

Fig. 6. Effect of phenolic combination and anti-diabetic drugs on lipid accumulation. Cells were treated as in Fig. 5C. (A) Effect on palmitate- or oleate-induced steatosis in HepG2 cells. Lipid accumulation was quantified by measuring the extracted dye at 490 nm. (B) Effect on intramyocellular lipids in insulin-resistant L6 cells. Palmitate-induced and serum-starved L6 myotubes were treated with DMSO (0.1 %, control), insulin (100 nM) or AICAR (2 mM) or metformin (1 mM) or combination of FER (25 μM) and RSV (10 μM) and EGCG (5 μM) for 15 min, and finally incubated in glucose-containing buffer for a further 4 h. Intramyocellular neutral lipid accumulation was determined by Oil Red O staining. Relative activity was calculated as the content of neutral lipid in test compound-treated L6 myotubes to that in insulin-treated cells. Data are shown as the mean ± SD form more than five independent experiments. Different superscript letters indicate significant differences at $p < 0.05$ using one-way ANOVA followed by the Tukey's *post hoc* comparison test.

supply to muscle and liver, which is correlated with the development of longer-term obesity-induced insulin resistance.[53] We demonstrated that the phenolic combination can facilitate a significant reduction in lipogenesis by adipose tissue as well as by the non-adipose tissue (Fig. 6A, 6B). Thus, this phenolic remedy can up-regulate glucose uptake and glycogen production while also reducing lipid content may contribute to successful long-term management of diabetes and obesity.

4. Conclusions

It is generally believed that the major tissues targeted by insulin's effects on metabolism include muscle, where insulin promotes glucose uptake; adipose tissue, where insulin inhibits lipolysis; and liver, where insulin promotes glucose utilization, suppresses glucose production, and promotes triglyceride synthesis.[1] Effects of the phenolic combination on glucose and lipid metabolism are summarized in Fig. 8. This phenolic combination appears to exert ameliorating effects to insulin resistance in a comprehensive manner. Besides, phytochemicals treatment might
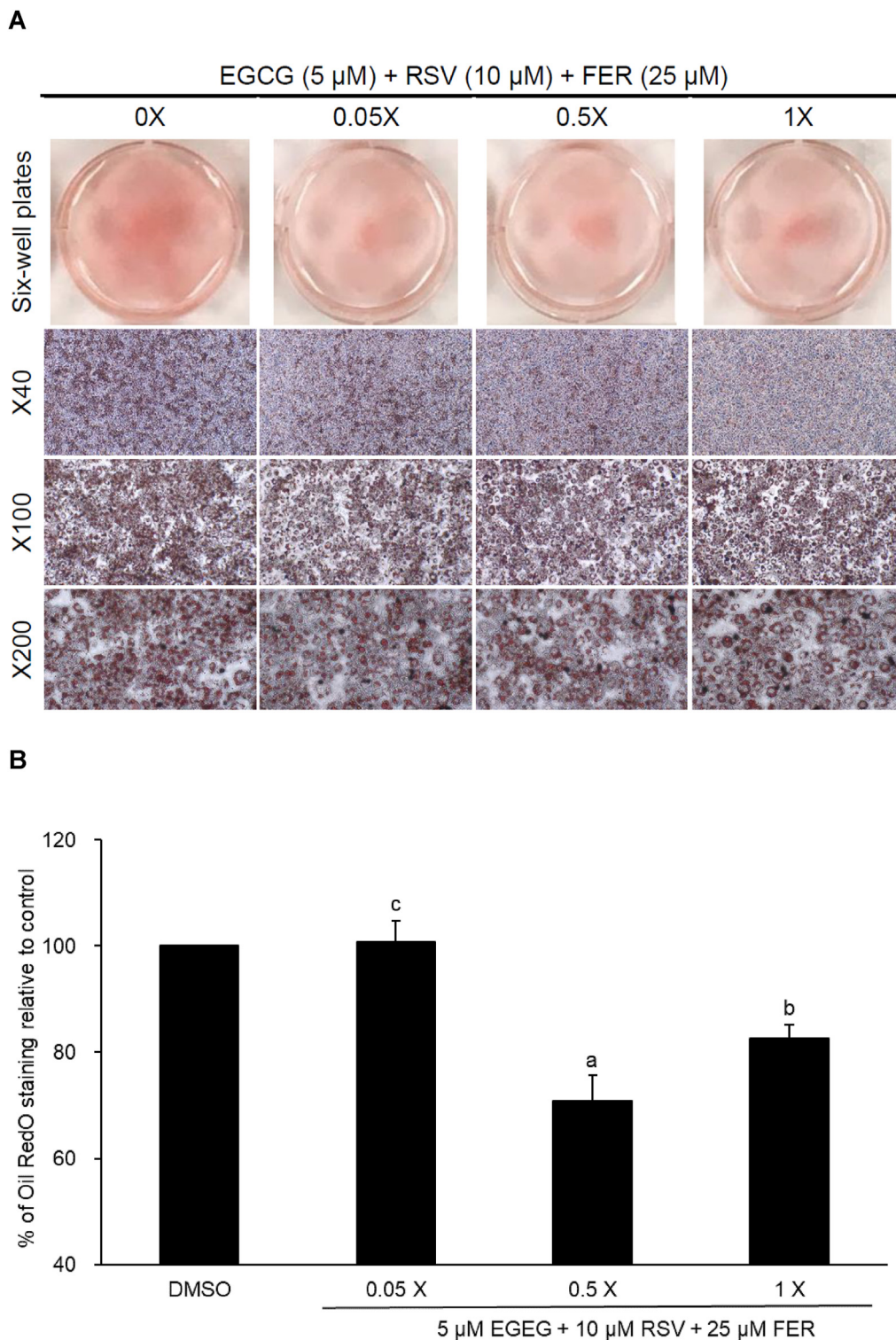
A

B

Fig. 7. Effect of phytochemical combination on differentiation of murine 3T3-L1 preadipocytes. (A) Photomicrographs of differentiating 3T3-L1 cells. Pictures are shown with three magnification factors ($\times$40, x100, and x200). (B) Treatment of pre-adipocytes (3T3-L1 cells) with a hormone inducer mixture for 8 days were differentiated to adipocytes. During differentiation, the cells were treated with the indicated concentration of phenolic combination every 3 days. Quantification of adipogenesis in 3T3-L1 cells by staining with ORO and measuring the absorbance of resolubilized ORO. The values were calculated as a % of the control cells treated with DMSO as a vehicle. Data are shown as the mean $+$SD form five independent experiments. Bars with different letters indicate statistical difference ($p < 0.05$) according to the Tukey's *post hoc* comparison test.

promote energy consumption with a reliance on glucose as primary source of energy. Therefore, the phenolic combination could probably contribute to the solution of T2DM in a systemic manifestation.

To the best of our knowledge, these findings serve as the first evidence that the combination with FER, RSV and EGCG has the ability to regulate glucose uptake, glycogen synthesis, glucose production and lipogenesis in peripheral tissues by promoting
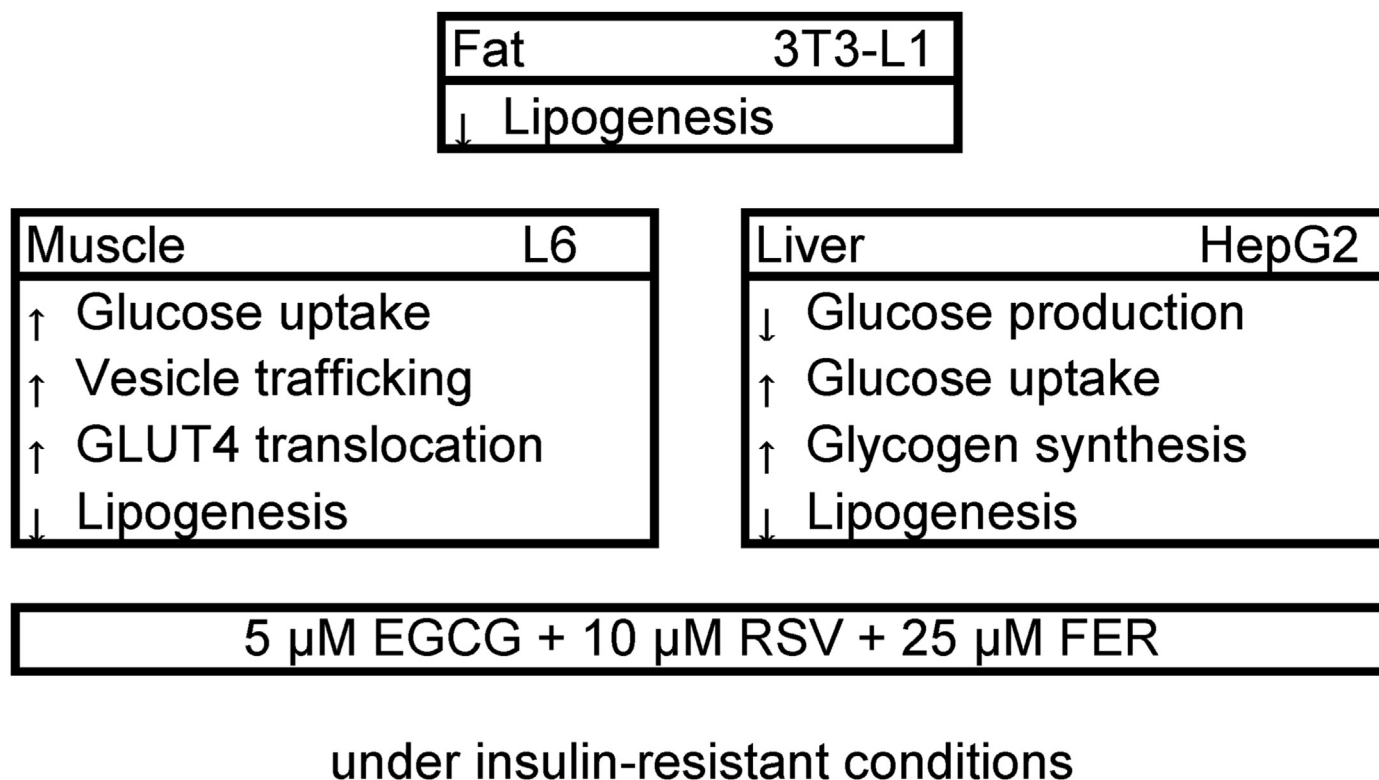
Fig. 8. Schematic describing the effects of phenolic combination in various tissues and cell types.

intracellular vesicle trafficking through simultaneous enhancement of insulin-independent biological actions. The three phenolic compounds may offer complementary adaptation solution to insulin resistance. More importantly, we observed the phenolic combination appears to be more efficacious than the current anti-diabetic drugs. Thus, they are promising compounds for the management of hyperglycemia and insulin resistance. However, future studies are needed to confirm the effect of phytochemical combination on glucose and lipid metabolism using animal model of obesity and diabetes.

Conflicts of interest statement

The authors declare no potential conflict of interest.

Acknowledgements

References

1. Haeusler RA, McGraw TE, Accili D. Biochemical and cellular properties of insulin receptor signalling. *Nat Rev Mol Cell Biol*. 2018;19:31—44. https://doi.org/10.1038/nrm.2017.89.
2. Affourtit C. Mitochondrial involvement in skeletal muscle insulin resistance: a case of imbalanced bioenergetics. *Biochim Biophys Acta*. 2016;1857:1678—1693. https://doi.org/10.1016/j.bbabio.2016.07.008.
3. Fruman DA, Chiu H, Hopkins BD, Bagrodia S, Cantley LC, Abraham RT. The PI3K pathway in human disease. *Cell*. 2017;170:605—635. https://doi.org/10.1016/j.cell.2017.07.029.
4. Li YQ, Shrestha YB, Chen M, Chanturiya T, Gavrilova O, Weinstein LS. Gsα deficiency in adipose tissue improves glucose metabolism and insulin sensitivity without an effect on body weight. *Proc Natl Acad Sci Unit States Am*. 2016;113:446—451. https://doi.org/10.1073/pnas.1517142113.
5. Boden G. Obesity, insulin resistance and free fatty acids. *Curr Opin Endocrinol Diabetes Obes*. 2011;18:139—143. https://doi.org/10.1097/med.0b013e3283444b09.
6. Teng H, Chen L. α-Glucosidase and α-amylase inhibitors from seed oil: a review of liposoluble substance to treat diabetes. *Crit Rev Food Sci Nutr*. 2017;57:3438—3448. https://doi.org/10.1080/10408398.2015.1129309.
7. Zabielski P, Chacinska M, Charkiewicz K, Baranowski M, Gorski J, Blachnio-Zabielska AU. Effect of metformin on bioactive lipid metabolism in insulin-resistant muscle. *J Endocrinol*. 2017;233:329—340. https://doi.org/10.1530/JOE-16-0381.
8. Koves TR, Ussher JR, Noland RC, et al. Mitochondrial overload and incomplete fatty acid oxidation contribute to skeletal muscle insulin resistance. *Cell Metabol*. 2008;7:45—56. https://doi.org/10.1016/j.cmet.2007.10.013.
9. Turban S, Stretton C, Drouin O, et al. Defining the contribution of AMP-activated protein kinase (AMPK) and protein kinase C (PKC) in regulation of glucose uptake by metformin in skeletal muscle cells. *J Biol Chem*. 2012;287:20088—20099. https://doi.org/10.1074/jbc.M111.330746.
10. Pei L, Yang J, Du J, Liu H, Ao N, Zhang Y. Downregulation of chemerin and alleviation of endoplasmic reticulum stress by metformin in adipose tissue of rats. *Diabetes Res Clin Pract*. 2012;97:267—275. https://doi.org/10.1016/j.diabres.2012.02.023.
11. Al Rashid MH, Majumder S, Mandal V, Mandal SC, Thandavarayan RA. In search of suitable extraction technique for large scale commercial production of bioactive fraction for the treatment of diabetes: the case Diospyros melanoxylon Roxb. *J Tradit Complement Med*. 2019;9:106—118. https://doi.org/10.1016/j.jtcme.2017.11.003.
12. Xiao J, So KF, Liong EC, Tipoe GL. Recent advances in the herbal treatment of non-alcoholic fatty liver disease. *J Tradit Complement Med*. 2013;3:88—94. https://doi.org/10.4103/2225-4110.110411.
13. Tadayon M, Movahedi S, Abedi P, Syahpoosh A. Impact of green tea extract on serum lipid of postmenopausal women: a randomized controlled trial. *J Tradit Complement Med*. 2018;8:391—395. https://doi.org/10.1016/j.jtcme.2017.07.005.
14. Chen L, Lin X, Fan X, et al. A self-emulsifying formulation of Sonchus oleraceus Linn for an improved anti-diabetic effect in vivo. *Food Funct*. 2020:1225—1229. https://doi.org/10.1039/c9fo00772e.
15. Chen L, Lin X, Teng H. Emulsions loaded with dihydromyricetin enhance its transport through Caco-2 monolayer and improve anti-diabetic effect in insulin resistant HepG2 cell. *J. Funct Foods*. 2020;64, 103672. https://doi.org/10.1016/j.jff.2019.103672.
16. Kang BB, Chiang BH. Amelioration of insulin resistance using the additive effect of ferulic acid and resveratrol on vesicle trafficking for skeletal muscle glucose metabolism. *Phytother Res*. 2020;34:808—816. https://doi.org/10.1002/ptr.6561.
17. Chen L, Teng H, Xie ZL, et al. Modifications of dietary flavonoids towards improved bioactivity: an update on structure-activity relationship. *Crit Rev*

Food Sci Nutr. 2018;58:513–527. https://doi.org/10.1080/10408398.2016.1196334.

18. Adisakwattana S. Cinnamic acid and its derivatives: mechanisms for prevention and management of diabetes and its complications. *Nutrients*. 2017;9:163–189. https://doi.org/10.3390/nu9020163.

19. de Melo TS, Lima PR, Carvalho KM, et al. Ferulic acid lowers body weight and visceral fat accumulation via modulation of enzymatic, hormonal and inflammatory changes in a mouse model of high-fat diet-induced obesity. *Braz J Med Biol Res*. 2017;50:e5630–e5637. https://doi.org/10.1590/1414-431x20165630.

20. Chen L, Teng H, Cao H. Chlorogenic acid and caffeic acid from Sonchus oleraceus Linn synergistically attenuate insulin resistance and modulate glucose uptake in HepG2 cells. *Food Chem Toxicol*. 2019;127:182–187. https://doi.org/10.1016/j.fct.2019.03.038.

21. Kang BB, Chiang BH. EGCG regulation of non-insulin-responsive endosomal compartments in insulin-resistant skeletal muscle. *Food Biosci*. 2019;28:1–6. https://doi.org/10.1016/j.fbio.2018.12.001.

22. Oshaghi EA, Goodarzi MT, Higgins V, Adeli K. Role of resveratrol in the management of insulin resistance and related conditions: mechanism of action. *Crit Rev Clin Lab Sci*. 2017;54:267–293. https://doi.org/10.1080/10408363.2017.1343274.

23. Isidoro C. Nutraceuticals and diet in human health and disease. The special issue at a glance. *J Tradit Complement Med*. 2020;10:175–179. https://doi.org/10.1016/j.jtcme.2020.06.002.

24. Kotzé-Hörstmann LM, Sadie-Van Gijsen H. Modulation of glucose metabolism by leaf tea constituents: a systematic review of recent clinical and pre-clinical findings. *J Agric Food Chem*. 2020;68:2973–3005. https://doi.org/10.1021/acs.jafc.9b07852.

25. Yao M, Teng H, Lv Q, et al. Anti-hyperglycemic effects of dihydromyricetin in streptozotocin-induced diabetic rats. *Food Sci Hum Well*. 2021;10:155–162. https://doi.org/10.1016/j.fshw.2021.02.004.

26. Sharma N, Arias EB, Sajan MP, et al. Insulin resistance for glucose uptake and Akt2 phosphorylation in the soleus, but not epitrochlearis, muscles of old vs. adult rats. *J Appl Physiol*. 2010;108:1631–1640. https://doi.org/10.1152/japplphysiol.01412.2009.

27. Huang L, Tepaamorndech S, Kirschke CP, et al. Aberrant fatty acid metabolism in skeletal muscle contributes to insulin resistance in zinc transporter 7 (Znt7)-knockout mice. *J Biol Chem*. 2018;293:7549–7563. https://doi.org/10.1074/jbc.M117.817692.

28. Gao D, Nong S, Huang X, et al. The effects of palmitate on hepatic insulin resistance are mediated by NADPH Oxidase 3-derived reactive oxygen species through JNK and p38MAPK pathways. *J Biol Chem*. 2010;285:29965–29973. https://doi.org/10.1074/jbc.M110.128694.

29. Fazakerley DJ, Naghiloo S, Chaudhuri R, et al. Proteomic analysis of GLUT4 storage vesicles reveals tumor suppressor candidate 5 (TUSC5) as a novel regulator of insulin action in adipocytes. *J Biol Chem*. 2015;290:23528–23542. https://doi.org/10.1074/jbc.M115.657361.

30. Tessneer KL, Jackson RM, Griesel BA, Olson AL. Rab5 activity regulates GLUT4 sorting into insulin-responsive and non-insulin-responsive endosomal compartments: a potential mechanism for development of insulin resistance. *Endocrinology*. 2014;155:3315–3328. https://doi.org/10.1210/en.2013-2148.

31. Martin LB, Shewan A, Millar CA, Gould GW, James DE. Vesicle-associated membrane protein 2 plays a specific role in the insulin-dependent trafficking of the facilitative glucose transporter GLUT4 in 3T3-L1 adipocytes. *J Biol Chem*. 1998;273:1444–1452. https://doi.org/10.1074/jbc.273.3.1444.

32. Yamamoto N, Ueda M, Sato T, et al. Measurement of glucose uptake in cultured cells. *Curr Protoc Pharmacol*. 2015;71:12–14. https://doi.org/10.1002/0471141755.ph1214s55.

33. Genovese S, Ashida H, Yamashita Y, et al. The interaction of auraptene and other oxyprenylated phenylpropanoids with glucose transporter type 4. *Phytomedicine*. 2017;32:74–79. https://doi.org/10.1016/j.phymed.2017.06.005.

34. Cicerchi C, Li N, Kratzer J, et al. Uric acid-dependent inhibition of AMP kinase induces hepatic glucose production in diabetes and starvation: evolutionary implications of the uricase loss in hominids. *Faseb J*. 2014;28:3339–3350. https://doi.org/10.1096/fj.13-243634.

35. Aydemir TB, Troche C, Kim MH, Cousins RJ. Hepatic ZIP14-mediated zinc transport contributes to endosomal insulin receptor trafficking and glucose metabolism. *J Biol Chem*. 2016;291:23939–23951. https://doi.org/10.1074/jbc.M116.748632.

36. Yoon SA, Kang SI, Shin HS, et al. p-Coumaric acid modulates glucose and lipid metabolism via AMP-activated protein kinase in L6 skeletal muscle cells. *Biochem Biophys Res Commun*. 2013;432:553–557. https://doi.org/10.1016/j.bbrc.2013.02.067.

37. Baskin KK, Winders BR, Olson EN. Muscle as a "mediator" of systemic metabolism. *Cell Metabol*. 2015;21:237–248. https://doi.org/10.1016/j.cmet.2014.12.021.

38. Jensen TE, Rose AJ, Hellsten Y, Wojtaszewski JFP, Richter EA. Caffeine-induced Ca2+ release increases AMPK-dependent glucose uptake in rodent soleus muscle. *Am J Physiol Endocrinol Metab*. 2007;293:E286–E292. https://doi.org/10.1152/ajpendo.00693.2006.

39. Kappel VD, Cazarolli LH, Pereira DF, et al. Involvement of GLUT-4 in the stimulatory effect of rutin on glucose uptake in rat soleus muscle. *J Pharm Pharmacol*. 2013;65:1179–1186. https://doi.org/10.1111/jphp.12066.

40. McConell GK, Ng GP, Phillips M, Ruan Z, Macaulay SL, Wadley GD. Central role of nitric oxide synthase in AICAR and caffeine-induced mitochondrial biogenesis in L6 myocytes. *J Appl Physiol*. 2010;108:589–595. https://doi.org/10.1152/japplphysiol.00377.2009.

41. Sadler JB, Bryant NJ, Gould GW, Welburn CR. Posttranslational modifications of GLUT4 affect its subcellular localization and translocation. *Int J Mol Sci*. 2013;14:9963–9978. https://doi.org/10.3390/ijms14059963.

42. Rudich A, Konrad D, Torok D, et al. Indinavir uncovers different contributions of GLUT4 and GLUT1 towards glucose uptake in muscle and fat cells and tissues. *Diabetologia*. 2003;46:649–658. https://doi.org/10.1007/s00125-003-1080-1.

43. Phadngam S, Castiglioni A, Ferraresi A, Morani F, Follo C, Isidoro C. PTEN dephosphorylates AKT to prevent the expression of GLUT1 on plasmamembrane and to limit glucose consumption in cancer cells. *Oncotarget*. 2016;7:84999–85020. https://doi.org/10.18632/oncotarget.13113.

44. Morani F, Phadngam S, Follo C, et al. PTEN regulates plasma membrane expression of glucose transporter 1 and glucose uptake in thyroid cancer cells. *J Mol Endocrinol*. 2014;53:247–258. https://doi.org/10.1530/JME-14-0118.

45. Treebak JT, Glund S, Deshmukh A, et al. AMPK-mediated AS160 phosphorylation in skeletal muscle is dependent on AMPK catalytic and regulatory subunits. *Diabetes*. 2006;55:2051–2058. https://doi.org/10.2337/db06-0175.

46. Larance M, Ramm G, Stockli J, et al. Characterization of the role of the Rab GTPase-activating protein AS160 in insulin-regulated GLUT4 trafficking. *J Biol Chem*. 2005;280:37803–37813. https://doi.org/10.1074/jbc.M503897200.

47. Yamamoto N, Sato T, Kawasaki K, Murosaki S, Yamamoto Y. A nonradioisotope, enzymatic assay for 2-deoxyglucose uptake in L6 skeletal muscle cells cultured in a 96-well microplate. *Anal Biochem*. 2006;351:139–145. https://doi.org/10.1016/j.ab.2005.12.011.

48. Randhawa VK, Bilan PJ, Khayat ZA, et al. VAMP2, but not VAMP3/cellubrevin, mediates insulin-dependent incorporation of GLUT4 into the plasma membrane of L6 myoblasts. *Mol Biol Cell*. 2000;11:2403–2417. https://doi.org/10.1091/mbc.11.7.2403.

49. Ishikura S, Koshkina A, Klip A. Small G proteins in insulin action: rab and Rho families at the crossroads of signal transduction and GLUT4 vesicle traffic. *Acta Physiol*. 2008;192:61–74. https://doi.org/10.1111/j.1748-1716.2007.01778.x.

50. Parafati M, Lascala A, Morittu VM, et al. Bergamot polyphenol fraction prevents nonalcoholic fatty liver disease via stimulation of lipophagy in cafeteria diet-induced rat model of metabolic syndrome. *J Nutr Biochem*. 2015;26:938–948. https://doi.org/10.1016/j.jnutbio.2015.03.008.

51. Czech MP. Insulin action and resistance in obesity and type 2 diabetes. *Nat Med*. 2017;23:804–814. https://doi.org/10.1038/nm.4350.

52. Samuel VT, Liu ZX, Qu X, et al. Mechanism of hepatic insulin resistance in nonalcoholic fatty liver disease. *J Biol Chem*. 2004;279:32345–32353. https://doi.org/10.1074/jbc.M313478200.

53. Turner N, Kowalski GM, Leslie SJ, et al. Distinct patterns of tissue-specific lipid accumulation during the induction of insulin resistance in mice by high-fat feeding. *Diabetologia*. 2013;56:1638–1648. https://doi.org/10.1007/s00125-013-2913-1.

54. Fullerton MD, Galic S, Marcinko K, et al. Single phosphorylation sites in Acc1 and Acc2 regulate lipid homeostasis and the insulin-sensitizing effects of metformin. *Nat Med*. 2013;19:1649–1654. https://doi.org/10.1038/nm.3372.

55. Zhou G, Myers R, Li Y, et al. Role of AMP-activated protein kinase in mechanism of metformin action. *J Clin Invest*. 2001;108:1167–1174. https://doi.org/10.1172/JCI13505.

56. Shaw RJ. Metformin trims fats to restore insulin sensitivity. *Nat Med*. 2013;19:1570–1572. https://doi.org/10.1038/nm.3414.

57. Li ZZ, Berk M, McIntyre TM, Feldstein AE. Hepatic lipid partitioning and liver damage in nonalcoholic fatty liver disease: role of stearoyl-CoA desaturase. *J Biol Chem*. 2009;284:5637–5644. https://doi.org/10.1074/jbc.M807616200.

58. Amati F, Dubé JJ, Alvarez-Carnero E, et al. Skeletal muscle triglycerides, diacylglycerols, and ceramides in insulin resistance: another paradox in endurance-trained athletes? *Diabetes*. 2011;60:2588–2597. https://doi.org/10.2337/db10-1221.

59. Kim JH, Mynatt RL, Moore JW, Woychik RP, Moustaid N, Zemel MB. The effects of calcium channel blockade on agouti-induced obesity. *Faseb J*. 1996;10:1646–1652. https://doi.org/10.1096/fasebj.10.14.9002558.

60. Prabhakar PK, Doble M. Interaction of phytochemicals with hypoglycemic drugs on glucose uptake in L6 myotubes. *Phytomedicine*. 2011;18:285–291. https://doi.org/10.1016/j.phymed.2010.06.016.

61. Haberland M, Carrer M, Mokalled MH, Montgomery RL, Olson EN. Redundant control of adipogenesis by histone deacetylases 1 and 2. *J Biol Chem*. 2010;285:14663–14670. https://doi.org/10.1074/jbc.M109.081679.